

High-Power Microstrip RF Switch

S. D. Choi

Telecommunications Division

A microstrip-type single-pole double-throw (SPDT) switch whose RF and bias portions contain only a metallized alumina substrate and two PIN diodes has been developed. It is superior to electromechanical and currently used circulator-type switches in many aspects of flight-qualified switch characteristics, such as power drain, weight, volume, magnetic cleanliness, cost, and reliability. A technique developed to eliminate the dc blocking capacitors needed for biasing the diodes is described. These capacitors are extra components and could lower the reliability significantly.

An SPDT switch fabricated on a 5.08- × 5.08- × 0.127-cm (2 × 2 × 0.050-in.)¹ substrate has demonstrated an RF power-handling capability greater than 50 W at S-band. The insertion loss is less than 0.25 dB and the input-to-off port isolation is greater than 36 dB over a bandwidth larger than 30 MHz. The input voltage standing-wave ratio is lower than 1.07 over the same bandwidth. Theoretical development of the switch characteristics and experimental results, which are in good agreement with theory, are presented in this article.

Introduction

Future space research will involve not only greater mission distances and durations but also more hostile environments. Successful completion of such missions requires improvement of the state-of-the-art in hardware design of the spacecraft radio system. RF switches, used for switching between antennas and redundant receivers, and transmitters should be extremely reliable and as simple and free from interfering with the rest of the system as possible. Although coaxial-type solid-state RF switches have been previously reported (References 1 and 2), they were not suited for high-power space applications. The PIN diodes used in these switches had inadequate power-handling capability and the coaxial switch circuits were subjected to

¹ Values in customary units are included in parentheses after values in SI (International System) units if the customary units were used in the measurements or calculations.

ionization breakdown at a relatively low power level. Recently, microstrip-compatible diodes with 1000-V reverse breakdown capability have become available. The microstrip-type solid-state diode switch reported here is superior to switch types currently used, such as the circulator and electromechanical types, in such aspects as power drain, weight, volume, magnetic cleanliness, cost, and reliability.

The basic concept of a diode switch is to transmit or reflect the RF power on a transmission line by means of altering the impedance states of one or more solid-state diodes. There are basically two switch types. In one type diodes are placed in shunt across the transmission line, while the other employs series diodes. Schematic drawings for the *on* and *off* modes of the two switch types are shown in Figure 1. For simplicity, the forward-biased switching element is represented with a short circuit and the reverse-biased element with an open circuit.

As is intuitively clear from the figure, the switching element in the series type should be able to handle the entire RF load power through the diode, whereas in the shunt type, the switching element experiences a fraction of the total power because the shunt stub serves as a transformer parallel to the main line. Although the series type is inherently wide band, the shunt type is usually superior to the series type in several important aspects of switch

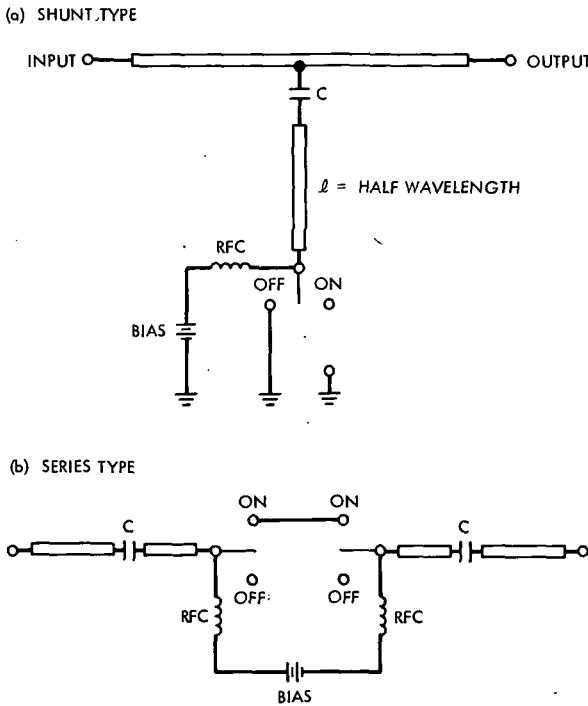


Figure 1. Switch types

characteristics, such as insertion loss, input-to-off port isolation, and power-handling capability.

In the shunt-type switch described in this article, a stub containing a switching diode is placed across a microstrip transmission line. When the switching diode is biased one way, the stub impedance at the main line is high and the RF power is unimpeded. Reversing the direction of the diode bias, the transmission line becomes shorted by a very low impedance presented by the stub. The number of the shunting stubs required in each arm of a switch is dictated primarily by the degree of isolation desired between the input and off port. The length and characteristic impedance of the stub are selected to yield optimum performance of the switch for a given set of diode parameters.

Presentation of the theoretical and measured result is preceded by brief characterizations of the switching element and the microstrip substrate.

PIN Diode and Microstrip Substrate

PIN diodes are exclusively employed as switching elements in solid-state RF switches because of their extremely high impedance under reverse-biased condition. In a PIN diode, highly doped p and n regions are separated by a layer of intrinsic semiconductor as shown in Figure 2. When the diode is forward-biased, carriers are injected into the intrinsic (I) region and it exhibits a very low impedance during the entire RF cycle. When the diode is reverse-biased, all the carriers in the I region are swept out and the I region appears as a low-loss dielectric. Therefore, the reverse-biased diode exhibits a much higher impedance than a reverse-biased ordinary pn junction diode. This is the outstanding feature of the PIN diode as a switching element. Electrical equivalent circuits and typical parameters for the device used are shown in Figure 2 and Table 1, respectively.

The microstrip circuits are fabricated on 1.27-mm (0.050-in.)-thick 99.5% pure alumina substrates with 0.05- μm surface finish on the circuit side and 0.25- μm finish on the ground plane side. Thickness of the gold metallization is 7.62 μm , which is about six times the skin depth at 2295 MHz. Relative permittivity and loss tangent of 99.5% pure alumina at 10 GHz are 9.7 and 0.0001, respectively. The dielectric loss and the conductor loss for 1.27-mm (0.050-in.)-wide transmission line at 2.3 GHz are calculated to be 5.1×10^{-4} dB/cm and 0.02 dB/cm, respectively. The adapter used between the microstrip line and the coaxial line (called the launcher) has an insertion loss of 0.02 dB at 2.3 GHz.

The calculated minimum insertion loss achievable with a 5.08-cm (2-in.)-long 50- Ω transmission line fabricated on this substrate material amounts to 0.15 dB, of which the conductor loss is predominant. A circuitry fabricated on a thicker substrate must have a wider, but not necessarily longer,

Table 1. Typical PIN diode parameters at 2295 MHz

Series resistance R_s	0.6 Ω	At +100 mA
Series inductance L_s	1.2 nH	(lead inductance)
Equivalent series resistance R_{sv}	1.8 Ω	At -200 V
Diode capacitance C_d	0.6 pF	At -200 V

metallization for a system having the same characteristic impedance. Therefore, the conductor loss can be reduced by using a thicker substrate. Further investigation is needed to determine the optimum thickness.

Single-Pole Single-Throw Switches

Schematic diagrams of the shunt stub switch are shown in Figure 3. Figure 3a shows a conventional microstrip switch configuration (Reference 2) in which a dc blocking capacitor is used. In this configuration one end of the diode is RF and dc grounded, which is usually accomplished by drilling a hole through the substrate for a ground post. The dc blocking capacitor is chosen so that, together with its series inductance, it is self-resonant at the band center frequency.

Figure 3b shows a new switch configuration which does not require the dc blocking capacitor or a ground post for the diode. Elimination of one capacitor and one ground post per stub could amount to considerable

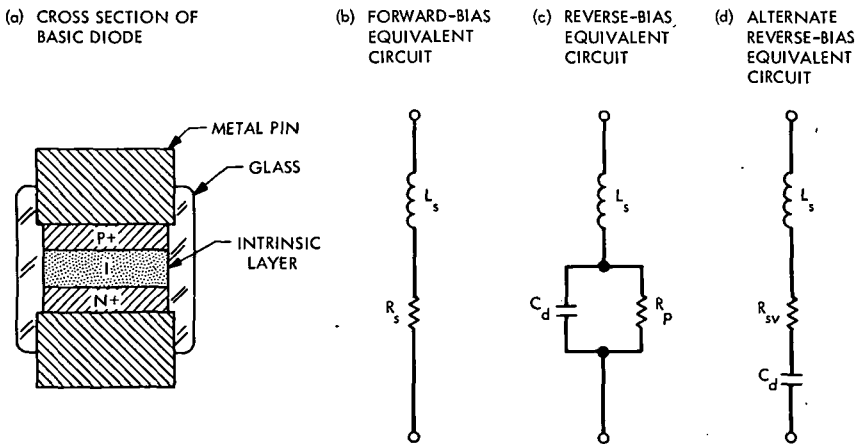
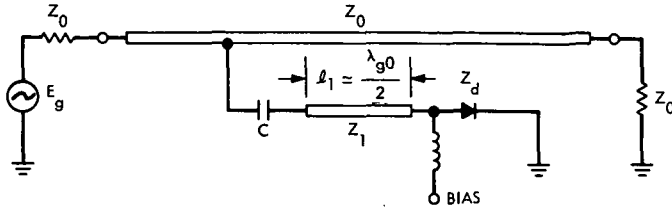


Figure 2. Equivalent circuits for PIN diodes

(a) HALF-WAVE STUB SWITCH WITH DC BLOCKING CAPACITOR



(b) SWITCH WITHOUT DC BLOCKING CAPACITOR

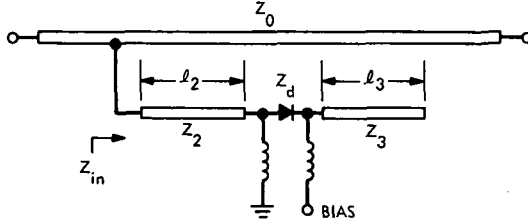


Figure 3. Schematic diagrams of the shunt stub SPST switches

improvement in reliability and ease of manufacturing for multipole switches.

The stub impedance seen by the main line, Z_{in} , is given by

$$Z_{in} = Z_2 \frac{(Z_3 \cos \phi_2 \cos \phi_3 - Z_2 \sin \phi_2 \sin \phi_3) + j(Z_d \cos \phi_2 \sin \phi_3)}{(-Z_d \sin \phi_2 \sin \phi_3) + j(Z_2 \cos \phi_2 \sin \phi_3 + Z_3 \sin \phi_2 \cos \phi_3)} \quad (1)$$

where

$$j = \sqrt{-1}$$

$$\phi_2 = \frac{2\pi}{\lambda_g} \ell_2$$

$$\phi_3 = \frac{2\pi}{\lambda_g} \ell_3$$

$$Z_d = \begin{cases} R_s + jX_L = \text{forward-biased diode impedance} \\ R_{sv} + j(X_L - X_C) = \text{reverse-biased diode impedance} \end{cases}$$

If the diode impedances in the forward- and reverse-biased states were purely real, the lengths of the stub segments, ℓ_2 and ℓ_3 in Figure 3b, should be one-quarter wavelength long at the band center frequency to make Z_{in} maximum for the switch on and Z_{in} minimum for the switch off. However, the impedances of practical diodes are complex as shown in Figure 2. Therefore, the segments are not exactly a quarter-wave long. But for convenience, such stubs are called quarter-wave stubs. For a quarter-wave stub the diode should be forward-biased to turn the switch on, and should be reverse-biased to turn it off.

It is important in a switch that the maximum and minimum stub impedances should occur at the band center frequency f_0 , so that the minimum insertion loss and the maximum isolation occur at this frequency. The condition which ensures this is obtained from Equation 1 by setting the imaginary part of the denominator and the real part of the numerator to zero for the switch on and off cases, respectively, and is (for the same characteristic impedances of the stub segments $Z_2 = Z_3$)

$$\left. \begin{aligned} Z_2(\tan \phi_{20} + \tan \phi_{30}) - X_{L0} \tan \phi_{20} \tan \phi_{30} &= 0 \\ Z_2(1 - \tan \phi_{20} \tan \phi_{30}) + (X_{C0} - X_{L0}) \tan \phi_{30} &= 0 \end{aligned} \right\} \quad (2)$$

where the subscript zero indicates the corresponding quantities evaluated at the band center frequency f_0 .

Solving Equation 2 for the stub lengths yields

$$\left. \begin{aligned} \phi_{20} &= \tan^{-1} \left[\frac{X_{C0}}{2Z_2} \pm \sqrt{\left(\frac{X_{C0}}{2Z_2}\right)^2 - 1} \right] \\ \phi_{30} &= \tan^{-1} \left[\frac{-\left(\frac{X_{C0}}{2Z_2} - \frac{X_{L0}}{Z_2}\right) \mp \sqrt{\left(\frac{X_{C0}}{2Z_2}\right)^2 - 1}}{1 - \frac{X_{C0}X_{L0}}{Z_2^2} + \left(\frac{X_{L0}}{Z_2}\right)^2} \right] \end{aligned} \right\} \quad (3)$$

The stub lengths in terms of quarter wavelength at the band center frequency ($\lambda_{g0}/4$) become

$$\left. \begin{aligned} \ell_2 &= \frac{2\phi_{20}}{\pi} \left(\frac{\lambda_{g0}}{4} \right) \\ \ell_3 &= \begin{cases} \frac{2\phi_{30}}{\pi} \left(\frac{\lambda_{g0}}{4} \right), & \text{if } \phi_{30} > 0 \\ 2 \left(1 + \frac{\phi_{30}}{\pi} \right) \left(\frac{\lambda_{g0}}{4} \right), & \text{if } \phi_{30} < 0 \end{cases} \end{aligned} \right\} \quad (4)$$

For a diode whose parameters are given in Table 1, the lengths become

$$\left. \begin{aligned} [\ell_2, \ell_3] &= \left[0.66 \left(\frac{\lambda_{g0}}{4} \right), 1.15 \left(\frac{\lambda_{g0}}{4} \right) \right] \\ \text{or} \\ [\ell_2, \ell_3] &= \left[0.34 \left(\frac{\lambda_{g0}}{4} \right), 1.59 \left(\frac{\lambda_{g0}}{4} \right) \right] \end{aligned} \right\} \quad (5)$$

for $Z_2 = Z_3 = 50\Omega$. It is clear that the lengths of the stub segments are quite different from a quarter wavelength. The first set of the stub segments in Equation 5 gives a shorter total length and it becomes for $\lambda_{g0}/4 = 1.27$ cm ($f_0 = 2295$ MHz), $[\ell_2, \ell_3] = [0.84$ cm, 1.46 cm]. Stubs are designed according to this formula and adjusted to yield the desired condition. The measured lengths were $[\ell_2, \ell_3] = [0.83$ cm, 1.46 cm], which are in good agreement with the theoretical values.

The insertion loss and isolation of the switch considering only diode impedance are given, respectively, by

$$\left. \begin{aligned} L_{\text{ins}} &= 20 \log \left| 1 + \frac{Z_0}{2Z_{\text{in(ON)}}} \right| \\ L_{\text{iso}} &= 20 \log \left| 1 + \frac{Z_0}{2Z_{\text{in(OFF)}}} \right| \end{aligned} \right\} \quad (6)$$

where $Z_{in(ON)}$ and $Z_{in(OFF)}$ are the stub impedances for switch on and off, respectively.

For a quarter-wave stub switch with diode parameters as given in Table 1, these are $L_{ins} = 0.039$ dB and $L_{iso} = 35.08$ dB at 2295 MHz. The measured insertion loss was 0.25 dB, which is the sum of losses due to launchers and main line (0.15 dB) and the stub (0.06 dB) and the mismatch loss of the stub (0.04 dB). The measured isolation was 34.2 dB. The theoretical and measured data are plotted in Figure 4 over a frequency range of 2.1 to 2.5 GHz.

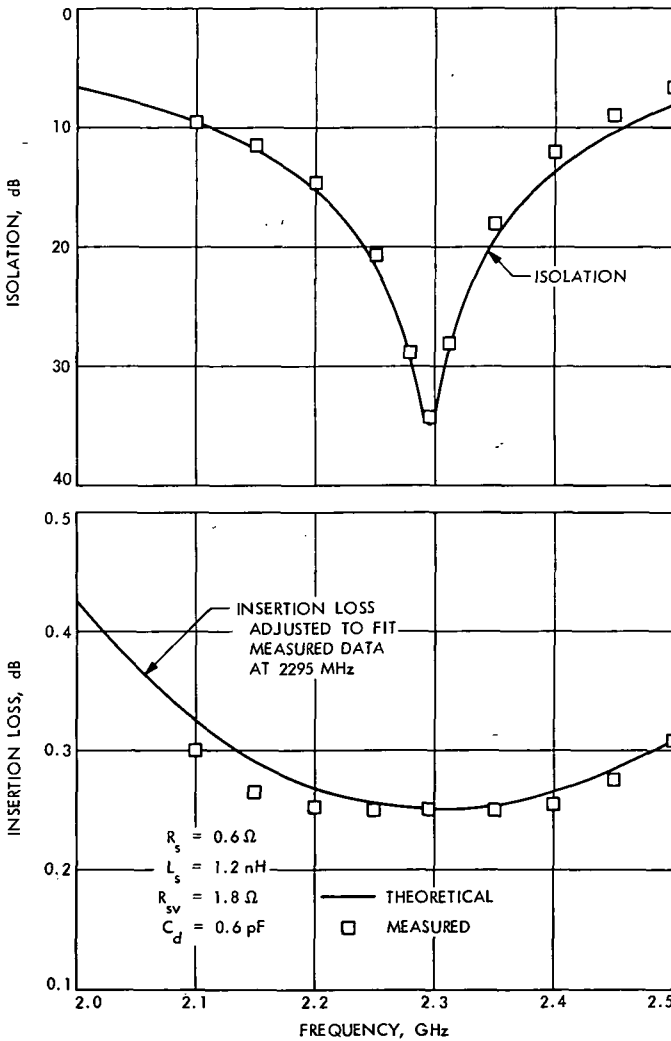


Figure 4. Insertion loss and isolation of SPST quarter-wave stub switch

Another possible configuration for this type of switch employs a stub segment whose length is on the order of one-half wavelength. For this configuration the diode should be reverse-biased to turn the switch on. This is just opposite to the condition for the switch using a quarter-wave stub. This is because a half-wave stub transforms an impedance into itself, whereas a quarter-wave stub transforms an impedance into a reciprocal of the impedance. Choice of one configuration over the other could depend on possible failure modes. For instance, if the failure mode of the diode is a short circuit, a half-wave stub switch will shut off that arm permanently, whereas the arm would be permanently on for a quarter-wave stub. Another important consideration in choosing the configuration is the fact that a half-wave stub switch has inherently narrower bandwidth than a quarter-wave stub switch.

Expressions for the input impedance and length of the stub at the band center frequency are listed in Table 2 for the quarter-wave and half-wave stubs. These equations illustrate which parameters of the diode are important in stub design.

Single-Pole Double-Throw Switch

A single-pole double-throw (SPDT) switch can be formed by combining two single-pole single-throw (SPST) switches. The bias arrangement should

Table 2. Input impedance and length of stubs

Parameter	Quarter-wave stub	Half-wave stub
$Z_{in(ON)}$	$\frac{Z_2 X_{C0}}{R_s \tan \phi_{20}}$	$-\frac{Z_2 X_{C0}}{R_{sv} \tan \phi_{20}}$
$Z_{in(OFF)}$	$\frac{Z_2 R_{sv}}{X_{C0} \tan \phi_{20}}$	$-\frac{Z_2 R_s}{X_{C0} \tan \phi_{20}}$
ϕ_{20}	$\tan^{-1} \left[\frac{X_{C0}}{2Z_2} \pm \sqrt{\left(\frac{X_{C0}}{2Z_2}\right)^2 - 1} \right]$	$\tan^{-1} \left[-\frac{X_{C0}}{2Z_2} \pm \sqrt{\left(\frac{X_{C0}}{2Z_2}\right)^2 - 1} \right]$
ϕ_{30}	$\tan^{-1} \left[\frac{-\left(\frac{X_{C0}}{2Z_2} - \frac{X_{L0}}{Z_2}\right) \mp \sqrt{\left(\frac{X_{L0}}{2Z_2}\right)^2 - 1}}{1 - \frac{X_{C0} X_{L0}}{Z_2} + \left(\frac{X_{L0}}{Z_2}\right)^2} \right]$	

be, of course, such that when one port is on, the other port is off. A photograph of a breadboard version of an SPDT switch is shown in Figure 5.

The insertion loss for the SPDT switch consists of the losses in the ON arm and the OFF arm. The insertion loss due to the forward-biased and reverse-biased diodes is given by

$$L_{\text{ins}} = 20 \log \left| 1 + \frac{Z_0}{2Z_{\text{in(ON)}}} + \frac{Z_{\text{in(OFF)}}}{2Z_0} \right| \quad (7)$$

The remainder of the insertion loss is contributed by the bias networks, the dielectric, and the conductors.

The isolation between the input and the off port for the SPDT switch is 6 dB better than for the SPST switch. This is because in the SPDT switch the incident RF current in the OFF arm is just one-half that in the SPST switch. The isolation is, therefore, given by

$$L_{\text{iso}} = 20 \log \left| 4 \left(1 + \frac{Z_0}{2Z_{\text{in(OFF)}}} \right) \right| \quad (8)$$

The insertion loss and isolation given by Equations 7 and 8 are plotted in Figure 6.

The measured data is plotted along with the theoretical curves in Figure 6. The insertion loss at the band center frequency was 0.25 dB. The measured data deviates from the theoretical curve less than 0.1 dB at 100 MHz away from the band center frequency. This discrepancy is believed to be due to neglecting the band limiting effect of the bias networks in the theoretical calculations. The measured data for the isolation agrees very well with the theoretical calculation. A summary of the performance of the SPDT switch is listed in Table 3.

Power and Vacuum Test

The SPDT switch shown in Figure 5 was subjected to a power test. The input power was raised in increments of 25 W up to a maximum of 100 W. The switch was allowed sufficient time to thermally stabilize at each power level. The temperature rise of the diode junction was 75°C above the ambient temperature at the 100-W level. According to the manufacturer's specifications, the diode can be safely operated with a junction temperature as high as 150°C.

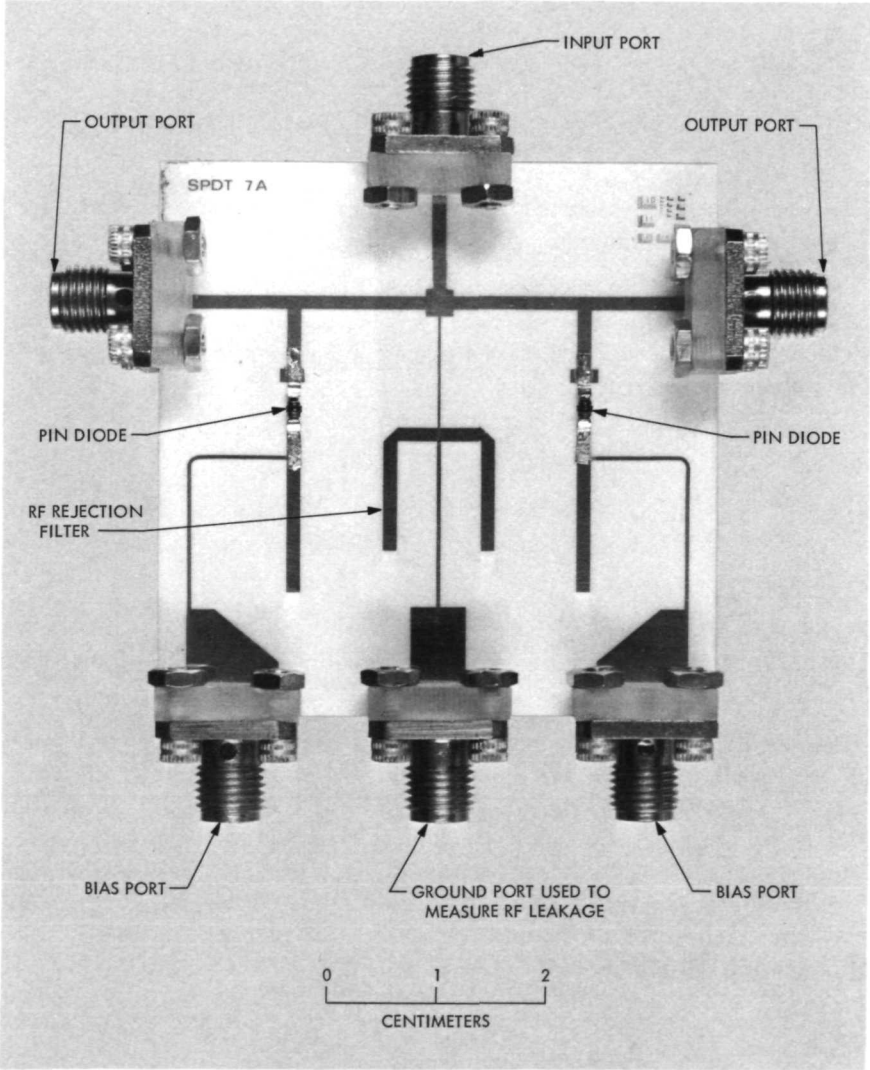


Figure 5. Breadboard SPDT switch

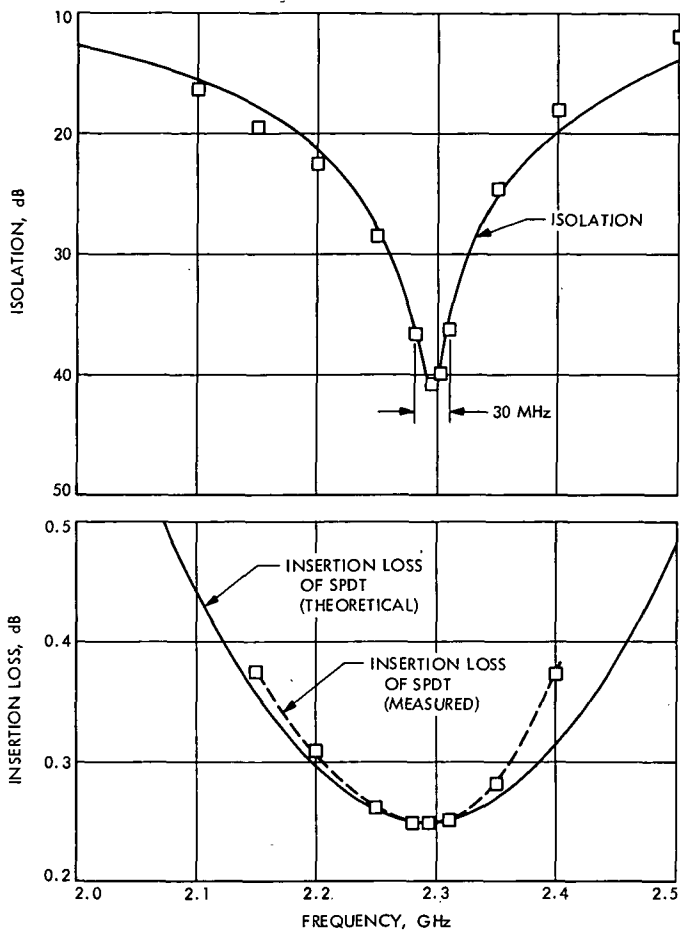


Figure 6. Insertion loss and isolation of SPDT quarter-wave stub switch

Table 3. Performance of SPDT switch

Band center frequency	2295 MHz
Input voltage standing-wave ratio	Lower than 1.07
Insertion loss	0.25 dB over 30 MHz
Isolation (minimum)	36 dB over 30 MHz
Input to bias port isolation	Greater than 45 dB

The power dissipation in the diode, P_D , is given by

$$P_D = \frac{R_s}{Z_0} P_L \quad (9)$$

where P_L is the power input to the switch. The power dissipated in the diode for $P_L = 100$ W is only 1.2 W. This indicates that the thermal resistance of the diode as mounted on the microstrip circuit is $62.5^\circ\text{C}/\text{W}$. The thermal resistance can be lowered by mounting the substrate on a solid metallic circuit frame and by using beryllium oxide dielectric directly beneath the diode.

The SPDT switch was also subjected to low-pressure tests. When operated at critical pressure [306.6 N/m² (2.3 torr)], ionization breakdown occurred at 150 W of RF power. Additional tests were performed at 533.3×10^{-5} N/m² (4×10^{-5} torr) to determine if multipacting breakdown would occur. None was observed for RF power levels as high as 150 W. According to published data (Reference 3), multipacting breakdown should not occur in this switch until 280 W.

Applications

The theory developed here can be easily adapted for the design of switches for many different applications. A few of the switch types which could be used for switching between antennas and redundant receivers and transmitters are illustrated in Figure 7, along with the matrices for the modes of operation and bias conditions. For the sake of simplicity, the stubs and diode bias networks are represented by diodes only.

These switches are combinations of SPST and SPDT switches. Therefore, the work presented in this article is the basic building block for many different switch types.

Summary and Conclusions

A microstrip type RF switch which uses only two PIN diodes on a microstrip substrate has been developed for application in spacecraft radio systems. An SPDT switch fabricated on a $5.08\text{-} \times 5.08\text{-} \times 0.127\text{-cm}$ ($2\text{-} \times 2\text{-} \times 0.05\text{-in.}$) alumina substrate can easily handle as much as 100 W of RF power. The insertion loss and isolation are better than 0.25 and 36 dB, respectively, over a 30-MHz band centered at 2295 MHz. This microstrip-type switch is superior to the currently used circulator and mechanical switches in terms of reliability, magnetic cleanliness, weight, volume, and power drain. A transfer switch is being made by combining two SPDT switches in parallel.

<u>SWITCH TYPE</u>	<u>SCHEMATIC DIAGRAM</u>	<u>MODE OF OPERATION</u>	<u>DIODE STATE*</u> A B C D
SPST		1-2 ON 1-2 OFF	F R
SPDT		1-2 ON } 1-3 OFF } 1-2 OFF } 1-3 ON }	F R R F
SP3T		1-2 ON 1-3 ON 1-4 ON	F R R R F R R R F
2P2T		1-3 ON 1-4 ON 2-3 ON 2-4 ON	F R F R F R R F R F F R R F R F
TRANSFER		1-3 } ON 2-4 } ON 1-4 } ON 2-3 } ON	R F R F F R F R

*DIODE STATES ASSUME QUARTER-WAVE STUBS. F AND R DESIGNATE FORWARD AND REVERSE BIASES, RESPECTIVELY.

Figure 7. Application of SPST and SPDT switches to form other switch types

Acknowledgment

The author wishes to express his appreciation to J. F. Boreham for his valuable advice and to J. H. Meysenburg for his contribution to this work.

References

1. White, J. F., and Mortenson, K. E., "Diode SPDT Switching at High Power with Octave Microwave Bandwidth," *IEEE Trans. Microwave Theory and Techniques*, Vol. MTT-16, pp. 30-36, Jan. 1968.
2. Watson, H. A., *Microwave Semiconductor Devices and Their Circuit Applications*, pp. 300-338. McGraw-Hill Book Co., Inc., New York, 1969.
3. Woo, R., *Final Report on RF Voltage Breakdown in Coaxial Transmission Lines*, Technical Report 32-1500. Jet Propulsion Laboratory, Pasadena, Calif., Oct. 1, 1970.